Finite Difference Solver for Modeling Shielding Gas Flow and Build Chamber Temperature in Metal Additive Manufacturing

A. Aatish Gupta,[1] B. Daniel Schicksnus,[1] and C. Karthik Subramaniam[1]
1. Carnegie Mellon University

I. ABSTRACT

Laser Powder Bed Fusion (LPBF) is a complex high energy process. The chamber must be flushed with an inert gas while the temperature around the build plate should remain relatively high to reduce residual stresses. To study the impact of inlet and outlet positions for the inert gas, a 2D CFD solver was developed using the Finite Difference Method to solve the incompressible conservative Navier-Stokes Equation. The matrix of cases evaluated showed us that an inlet near the bottom of the chamber and an outlet near the top of the chamber (heights of 0.0 - 0.1 m and 0.3 - 0.4 m, respectively) provided the best balance between flow and heat conservation.

II. INTRODUCTION

Additive Manufacturing has been progressing rapidly over the last decade, especially Laser Powder Bed Fusion (LPBF). With the large number of new companies that are manufacturing machines and trying to optimize and scale the process for mass manufacturing, it is vital to understand how to make the process safe and free from defects. To achieve these goals, optimizing the flow inside the chamber is essential.

The inert gas flow serves multiple purposes, namely: removing Oxygen from the chamber to prevent combustion and oxidation of the metal build material, carrying spatter particles away from the build area and from the laser, and convecting heat away from the build plate. Spatter particles are half melted metal powder particles that shoot off a melt pool (the point of contact between the laser and the powder bed). These spatter particles can affect the quality of the build or even damage the laser of the machine. We also care about how much heat the inert gas convects away from the build plate as the background temperature of a build is the biggest indicator of the magnitude of residual stresses inside of the build part. As such we want to have a high temperature around the build plate to ensure that the part being printed is defect free.

Weaver et al.[1] performed experiments to show a developed flow and measure the speeds of the inert gas flow in Laser Powder Bed Fusion. They used schlieren imaging and hot film anemometer to both qualitatively and quantitatively describe the flow in EOS' M290 commercial LPBF machine. This machine mas multiple inlet pores spaced close to each other. Thus, even if each individual flow has a parabolic flow field, the cumulative flow field of the inlet will be more or less constant. They also measured the inlet velocity to be 4m/s. Anwar et al.[2] performed simulations to model spatter transport and concluded that a flow of around 2 m/s over the build plate is necessary to ensure the quality of the build by removing spatter particles from the powder bed. They also demonstrated the behaviour of higher energy particles near the laser. D'Amicio et al.[3] performed FEA simulations of extrusion-based Additive processes and showed that a thermal gradient is the main cause of residual stress in Additive Manufacturing. Li et al.[4] also demonstrated post-processing and in situ process control measures to reduce residual stresses which are also thermal in nature. Based on our review of the literature, we can see that the largest indicator of the residual stresses in an additively manufactured part is the temperature from which the part is uniformly cooled. If the temperature in the chamber is high enough, almost no post processing will be necessary to get a high quality part after the build is complete.

Patents of Additive manufacturing machines have similar configurations to the one studied in our model, with the inlet and outlet position varying[5]. This report aims to solve the incompressible, conservative form of the 2D Navier-Stokes equation to model the effects of varying inlet and outlet positions of the inert shielding gas flow in a LPBF machine on chamber temperature and gas velocity. The inert shielding gas most often used in commercial applications is argon, so coefficients and properties similar to those of argon were considered. An optimal configuration for build quality based on our findings is reported.

III. METHODS

A. Problem setup

To tackle this problem, a CFD solver was written in Python using NumPy[6] to solve the conservative form of Navier-Stokes using the Finite Difference Method. The Navier-Stokes equation is made up of two parts, the first being the continuity equation:

$$\frac{\partial(u)}{\partial x}+\frac{\partial(v)}{\partial y}=0 \tag{1}$$

where u and v are the x and y components of the velocity vector $\vec{u}$ respectively. The second are the momentum equations:
Momentum equation in x-direction

$$\frac{\partial v}{\partial t}+\frac{\partial uu}{\partial x}+\frac{\partial vu}{\partial y}=-\frac{1}{\rho}\frac{\partial p}{\partial y}+\nu\left(\frac{\partial^2 v}{\partial x^2}+\frac{\partial^2 v}{\partial y^2}\right) \tag{2}$$

Momentum equation in y-direction

$$\frac{\partial u}{\partial t}+\frac{\partial uv}{\partial x}+\frac{\partial vv}{\partial y}=-\frac{1}{\rho}\frac{\partial p}{\partial x}+\nu\left(\frac{\partial^2 u}{\partial x^2}+\frac{\partial^2 u}{\partial y^2}\right) \tag{3}$$

The considered domain consists of a 0.4m x 0.4m 2D grid. A preliminary analysis was done using a 20 x 20 mesh grid to test the different inlet and outlet positions and find an area of interest for a more in-depth analysis. The subsequent analysis was done using a 40 x 40 mesh grid for the case identified to be the best based on the results of the preliminary analysis. This was done as solving the model on a finer mesh took an order of magnitude longer than solving on the coarser mesh. The velocity was solved on a staggered grid, and the solution was interpolated to calculate the temperature on a collocated grid.

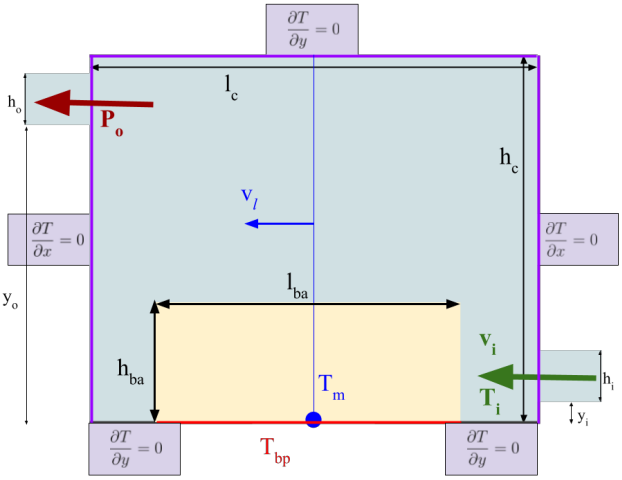

FIG. 1. Schematic of the domain with flow and temperature boundary conditions

To solve the Navier stokes equations we used the Fractional Step Method. It is a semi-implicit method that uses the Picard linearization. This means that the diffusive term is solved implicitly using the Crank-Nicolson method and the advective term is solved explicitly using the Adams-Bashforth approximation. As our domain has a length of 0.4 m and our inlet flow has a velocity of 4 m/s we assume that a steady state flow is reached after one second.
To calculate the Temperature Advection-Diffusion, a blended-scheme of second order, consisting of both upwind and central discretizations, was implemented on a collocated grid with the advection velocities being the steady state flow velocities u and v calculated before. As these velocities can be quite low we ran the scheme for ten seconds to retrieve a near steady state temperature field.

$$\frac{\partial T}{\partial t}+u\frac{\partial T}{\partial x}+v\frac{\partial T}{\partial y}=\alpha\left(\frac{\partial^2 T}{\partial x^2}+\frac{\partial^2 T}{\partial y^2}\right) \tag{4}$$

The physical properties of Argon that have been tried can be seen in Table 1. However, to ensure stability especially during the windup phase, the timestep would have to be reduced to the order of nanoseconds to solve the problem with the correct viscosity and thermal diffusivity of Argon. As these computations were to costly to evaluate on the resources available to us we increased the viscosity and thermal diffusivity to avoid instabilities for the lowest feasible timestep given the circumstances. The conclusions drawn should not be widely different, but a validation using the correct material properties might be necessary before implementing our results directly for gases with dissimilar parameters.

Property	**Value**
Density [$\frac{kg}{m^3}$]	1.633
Dynamic Viscosity [Pa·s]	3.77×10^{-5}
Specific Heat Capacity [$\frac{J\cdot K}{kg}$]	520
Thermal Diffusivity	2.2×10^{-5}

TABLE I. Physical Properties of Argon.

B. Discretized Equations

We can discretize the Navier-Stokes equation as follows -

$$u^*_{i,j}=u^n_{i,j}+\Delta t\left[-A^n+B^n\right] \tag{5}$$

Where A^n is the Convective term and B^n is the Diffusive term in the Navier-Stokes momentum equation, and u^* is an intermediate velocity calculated implicitly while ignoring the effect of pressure. We used the iterative Point Jacobi method to find the pressure values.

$$P^{(n+1)}_{i,j}=(\frac{1}{4}\left(P^{(n+1)}_{i-1,j}+P^{(n+1)}_{i,j-1}+P^{(n+1)}_{i+1,j}+P^{(n+1)}_{i,j+1}\right)-\frac{h^2}{4}\nabla\cdot u^*) \tag{6}$$

$$u^{(n+1)}_{i,j}=u^*_{i,j}-\frac{\Delta t}{\rho}(\nabla p^{(n+1)}) \tag{7}$$

We can discretize the Advection Diffusion equation used in to find the chamber temperature using an upwind/central blended scheme of second order with q = 0.25:

$$u^+=max(u^{(n)}_{i,j},0) \tag{8}$$

$$u^-=min(u^{(n)}_{i,j},0) \tag{9}$$

$$v^+=max(v^{(n)}_{i,j},0) \tag{10}$$

$$v^-=min(v^{(n)}_{i,j},0) \tag{11}$$

$$T^-_x=\frac{T^{(n)}_{i-2,j}-3T^{(n)}_{i-1,j}+3T^{(n)}_{i,j}-T^{(n)}_{i+1,j}}{3\Delta x} \tag{12}$$

$$T_x^+ = \frac{T_{i-1,j}^{(n)} - 3T_{i,j}^{(n)} + 3T_{i+1,j}^{(n)} - T_{i+2,j}^{(n)}}{3\Delta x} \tag{13}$$

$$T_y^- = \frac{T_{i,j-2}^{(n)} - 3T_{i,j-1}^{(n)} + 3T_{i,j}^{(n)} - T_{i,j+1}^{(n)}}{3\Delta y} \tag{14}$$

$$T_y^+ = \frac{T_{i,j-1}^{(n)} - 3T_{i,j}^{(n)} + 3T_{i,j+1}^{(n)} - T_{i,j+2}^{(n)}}{3\Delta y} \tag{15}$$

$$\begin{aligned}
&\frac{T_{i,j}^{(n+1)} - T_{i,j}^{(n)}}{\Delta t} \\
&+ u_{i,j}^{(n)} \left(\frac{T_{i+1,j}^{(n)} - T_{i-1,j}^{(n)}}{2\Delta x} \right) + q[u^+ w_x^- + u^- w_x^+] \\
&+ v_{i,j}^{(n)} \left(\frac{T_{i,j+1}^{(n)} - T_{i,j-1}^{(n)}}{2\Delta y} \right) + q[v^+ w_y^- + v^- w_y^+] \\
&= \alpha \left(\frac{T_{i+1,j}^{(n)} - 2T_{i,j}^{(n)} + T_{i-1,j}^{(n)}}{\Delta x^2} + \frac{T_{i,j+1}^{(n)} - 2T_{i,j}^{(n)} + T_{i,j-1}^{(n)}}{\Delta y^2} \right)
\end{aligned} \tag{16}$$

C. Boundary Conditions

The inlet and outlet heights were tested over a range of 0.4 m for 0.1 m increments on the coarse mesh. They were incremented by 0.05 m on the fine mesh. There were two sets of boundary conditions used, one for the full Navier Stokes analysis and the second for the Advection Diffusion analysis used to model the temperature.

For the full Navier stokes, the inlet velocity was set to 4m/s and the outlet pressure was set to ambient pressure. The boundary condition at the inlet (j > inlet height and j < inlet height + inlet size (0.1 m)) was a Dirichlet condition:

$$u_{0,j} = 4m/s$$

The boundary condition at the outlet (j > outlet height and j < outlet height + inlet size (0.1 m)) was a Neumann condition:

$$\frac{\partial u_{0,j}}{\partial y} = 0$$

The boundary conditions for the rest of the domain were Dirichlet no-slip condition where all velocities were set to zero. The interior points were also set such that the interpolation between the boundary adjacent points and the ghost nodes were equal to zero.

$$\begin{aligned} u_{boundary} &= 0 \\ v_{boundary} &= 0 \end{aligned} \tag{17}$$

For the temperature boundary conditions all insulated walls had Neumann conditions such that

$$\begin{aligned} \frac{\partial T}{\partial x} &= 0 \\ \frac{\partial T}{\partial y} &= 0 \end{aligned} \tag{18}$$

The temperature boundary conditions at the inlet (19), build plate (20) ((l > 0.073 m and l < 0.327 m), and melt point (21) (l = 0.2 m) were Dirichlet conditions:

$$T_{0,j} = 350K \tag{19}$$

$$T_{l,0} = 473K \tag{20}$$

$$T_{l,0} = 1700K \tag{21}$$

D. Goal Metrics

The flow has been quantitatively classified to determine which configurations have a desirable flow field. Any cases where the average gas speed in a 0.1 m space over the build plate was less than 2 m/s were considered to be infeasible as the velocity would not suffice to clear the spatter. Flows with higher average speeds were thus preferred. For a visual reference, the evaluation region is indicated in yellow in Figure 1. Similarly, the mean of the temperatures in the same surrounding area of the build plate were considered as the background temperature. We used these metrics in both the preliminary and final analyses.

IV. RESULTS

A. Coarse Mesh

For the preliminary analysis, sixteen cases were run and the results of the velocity and temperature solutions can be seen in Figures 3 and 4. The scores assigned to these cases are presented in Figure 5. We used the following scoring method to determine the best case, where the weighting coefficients were chosen as a heuristic. All cases where the average velocity over the build area was less than 2 m/s were assigned a score of zero.

$$Score = 0.1 * (T_{avg} - T_{min}) + 0.5 * (S_{avg} - S_{min}) \tag{22}$$

- T_{avg} Average temperature (K)
- T_{min} Minimum temperature (450 K)
- S_{avg} Average speed (m/s)
- S_{min} Minimum speed (2 m/s)

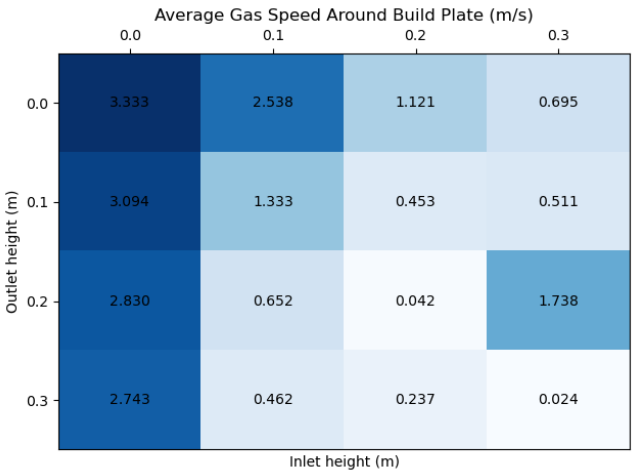

FIG. 2. Mean flow velocities for preliminary cases

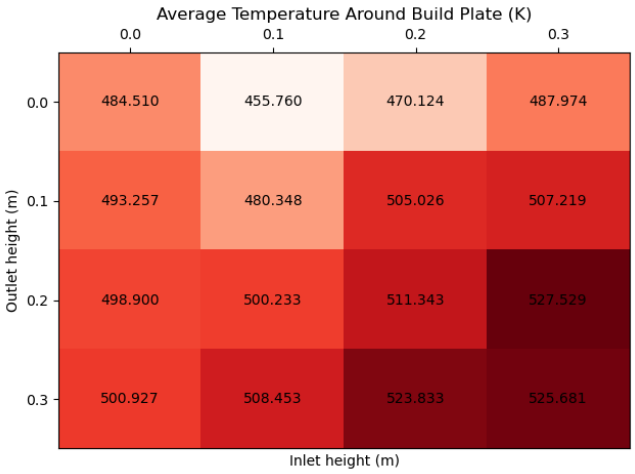

FIG. 3. Mean temperatures for preliminary cases

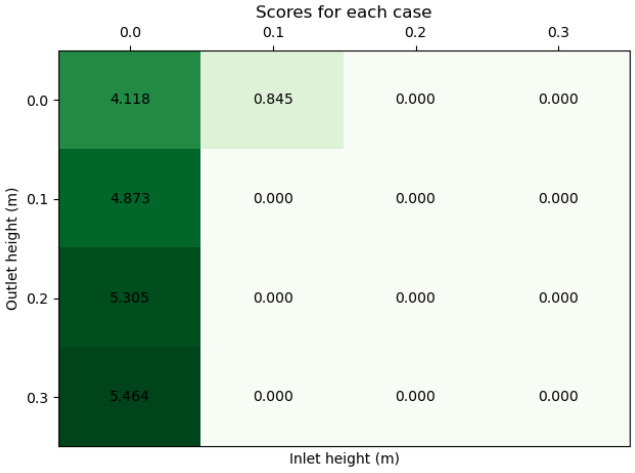

FIG. 4. Scores for preliminary cases

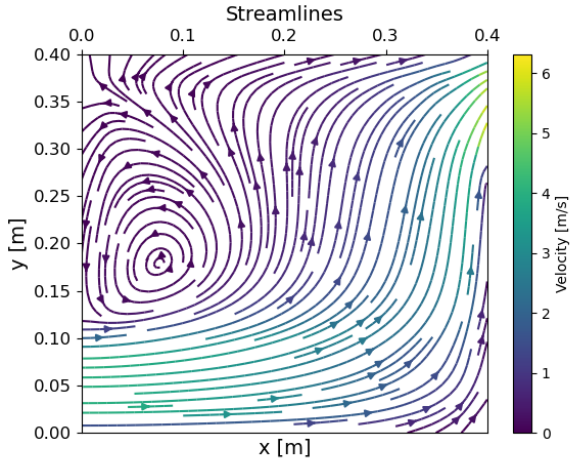

FIG. 5. Stream Plot for Best Case (Inlet: 0.0, Outlet: 0.3)

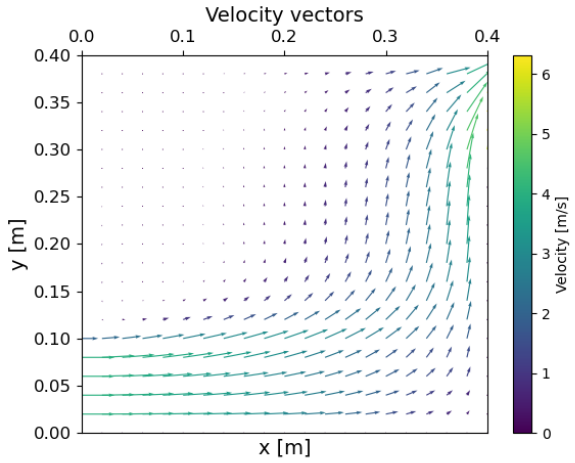

FIG. 6. Velocity Vectors for Best Case (Inlet: 0.0, Outlet: 0.3)

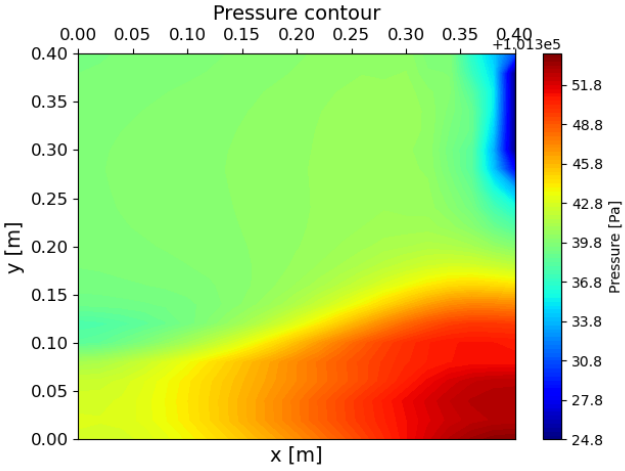

FIG. 7. Pressure Contours for Best Case (Inlet: 0.0, Outlet: 0.3)

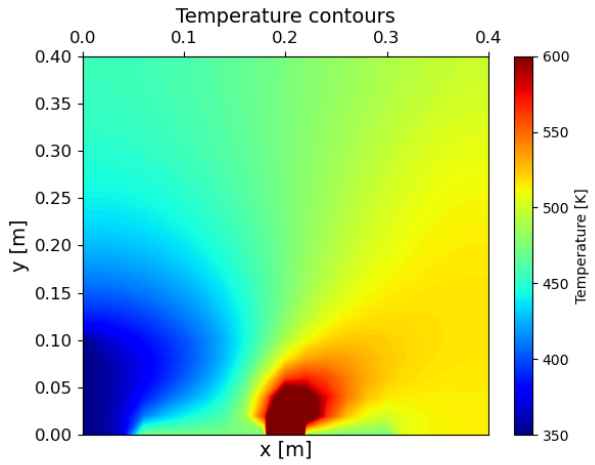

FIG. 8. Temperature Contours for Best Case (Inlet: 0.0, Outlet: 0.3)

We can see from Figure 4 that the inlet at height 0.0 m and outlet at height 0.3 m gave us the highest score. Examining figures 2 and 3 shows us that this case does not have the highest temperature or speed, but offers a good mix of both. The streamline, velocity vector, pressure, and temperature plots for the optimal case are shown in figures 5-8.

An example of a case (Inlet:0.2, Outlet:0.3) with high mean temperature without adequate flow over the build plate to carry away spatter is shown in Figures 9 and 10.

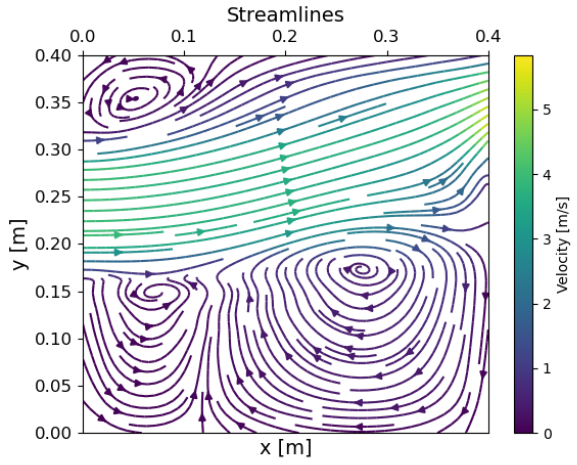

FIG. 9. Inadequate flow in build area (Inlet:0.2, Outlet:0.3)

We can see that due too the low velocity there is no great affect on the temperature, likely because the temperature diffusivity of Argon is so low. This would be ideal for a high background temperature, but as the spatter can not be carried away this case is infeasible.

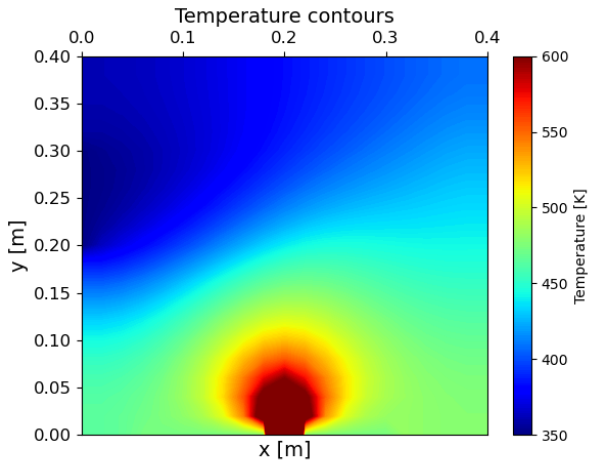

FIG. 10. High mean temperature in build area (Inlet:0.2, Outlet:0.3)

B. Fine Mesh

We examined cases around the best case from the preliminary analysis, with the inlet at height 0.0 m and outlet at height 0.3 m, on a finer mesh. The average temperatures, velocities, and scores are reported in figures 11-13.

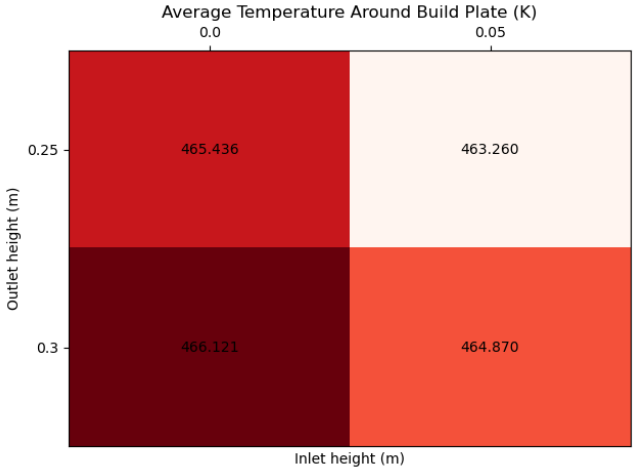

FIG. 11. Mean temperatures for final analysis

We note that changing the mesh size to be finer somewhat changed the dynamics of the problem. The melt point became smaller with respect to the chamber on the finer mesh than it was on the coarse mesh. This led to the overall temperature in the chamber being lower on the fine mesh. Additionally, refining the mesh led to more accurate velocity results, which lowered the average speeds. The result is that the scores for the finer mesh are not comparable against those of the coarse mesh, only to each other. After taking this into consideration, the fine mesh analysis still supported that a configuration with an inlet height of 0.0 m and 0.3 m was the best case. Only the vector and temperature plots from the finer mesh are shown

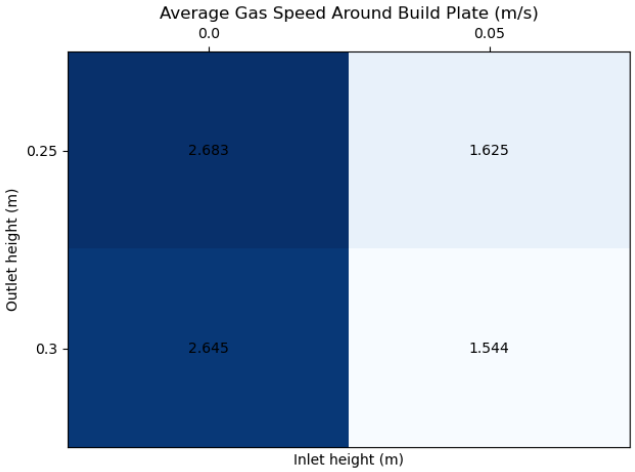

FIG. 12. Mean flow speeds for final analysis

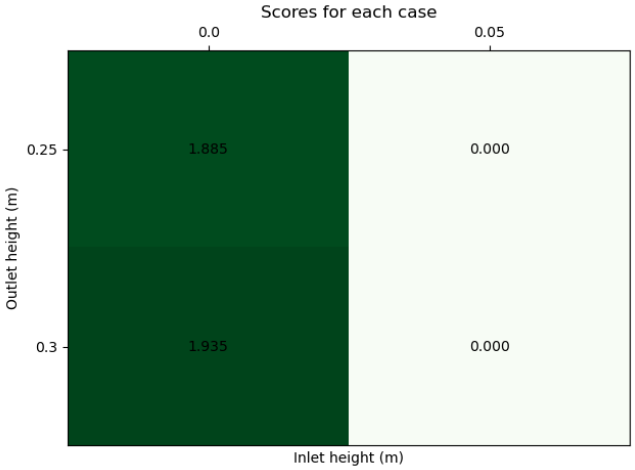

FIG. 13. Scores for final analysis

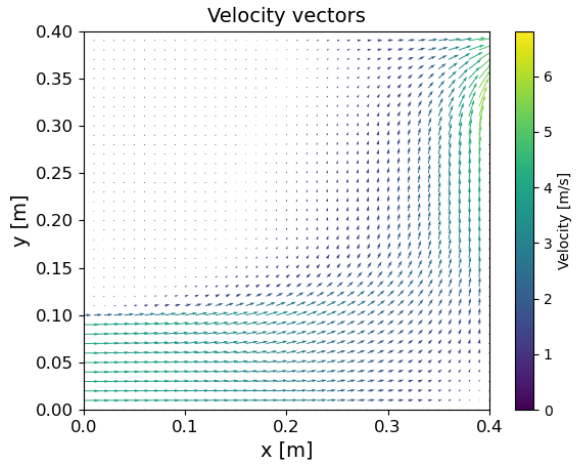

FIG. 14. Velocity Vectors for Case (Inlet: 0.0, Outlet: 0.3)

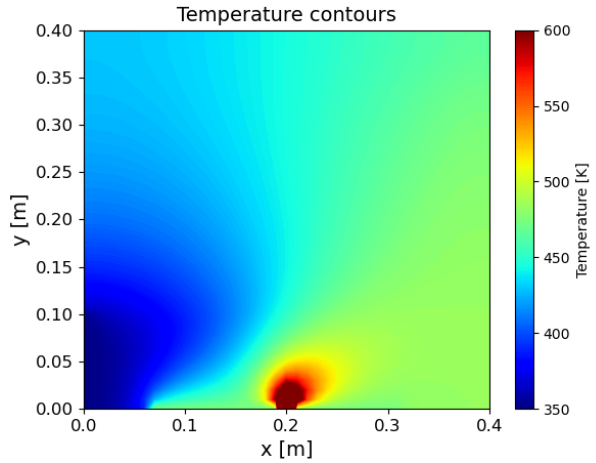

FIG. 15. Temperature Contours for Case (Inlet: 0.0, Outlet: 0.3)

(Figures 14 and 15) because the other plots look almost identical to the plots given by the coarse mesh analysis.

V. DISCUSSION

One big drawback of the formulation used in this project is the lack of eddy currents formed, which might be a result of the changes to the dynamic viscosity. Moving forward, a multiple inlet, multiple outlet configuration could also be considered to ensure that the entire domain gets flushed with Argon and to protect the laser from spatter reaching the top of the domain. Although the uniformity of the temperature of the build plate was initially considered to be significant, the standard deviation of the temperature around the build plate has not been considered as a goal metric. Since the laser is stationary in our domain and we are taking the temperature distribution at a snapshot in time, the heat will be concentrated just over the melt point. However, in a real machine setup, the melt point will move around the build plate. This will result in a more even temperature distribution that cannot be captured by our simulation setup. Figure 8 demonstrates this melt point on a temperature contour on our coarse mesh.

Both our preliminary and final analyses revealed that the optimal inlet and outlet heights are flush with the bottom and top of the chamber, respectively. This configuration allows for both fast gas flow over the build plate to carry away spatter particles and a high temperature to prevent residual stresses in the AM part.

One thing to note is that we had to increase the nu value of Argon by several orders of magnitude to prevent the simulation from blowing up. While our model may not reflect the real world with a high degree of accuracy due to this factor, the flows are still viable for comparison to one another and for other inert gases with similar parameters.

A. Future Work

Future work would use higher compute power and more time to run the simulations so as to reduce the viable timestep to the order of nanoseconds. This would allow us to model the true nu value of Argon and give us more accurate results. More involved setups to be considered are one with multiple inlets and or multiple outlets, or one with dispersed inlets rather than continuous ones.

VI. CONTRIBUTIONS

The Navier-Stokes solver was written, and the experiment was designed by Karthik Subramaniam.
Aatish Gupta wrote the Point Jacobi Iteration and the Case Evaluation Script.
Daniel Schicksnus wrote the Temperature solver, the Navier-Stokes boundary conditions, and ran the case evaluations.
All group members contributed to running and debugging the code in various iterations, discussing the code and setup, and writing the report.
Together with the report, we submit the code used to evaluate the mentioned case studies, as well as the results saved in .npy matrices and the corresponding plots.

REFERENCES

[1] J. S. Weaver, A. Schlenoff, D. C. Deisenroth, and S. P. Moylan, "Inert gas flow speed measurements in laser powder bed fusion additive manufacturing," NIST Advanced Manufacturing Series **100**, 43 (2021).
[2] A. B. Anwar, I. H. Ibrahim, and Q.-C. Pham, "Spatter transport by inert gas flow in selective laser melting: A simulation study," Powder Technology **352**, 103–116 (2019).
[3] A. D'Amico and A. M. Peterson, "An adaptable fea simulation of material extrusion additive manufacturing heat transfer in 3d," Additive Manufacturing **21**, 422–430 (2018).
[4] C. Li, Z. Liu, X. Fang, and Y. Guo, "Residual stress in metal additive manufacturing," Procedia Cirp **71**, 348–353 (2018).
[5] M. Sweetland, "Additive manufacturing system with gas flow head," (2022), uS Patent 11,453,087.
[6] T. E. Oliphant *et al.*, *Guide to numpy*, Vol. 1 (Trelgol Publishing USA, 2006).